A pentacene-silicon heterojunction with multiple functions

Jung-Hun Seo[1†], Tea-Yeon Oh[2†], Jungho Park[2], Weidong Zhou[3], Byeong-kwon Ju[2] and Zhenqiang Ma[1*]

[1] Department of Electrical and Computer Engineering, University of Wisconsin-Madison, Madison, Wisconsin 53706, USA

[2] Display and nanosystem laboratory, School of Engineering, Korea University, Seoul, 136-713, Republic of Korea

[3] Department of Electrical Engineering, NanoFAB Center, University of Texas at Arlington, Arlington, Texas 76019, USA

ABSTRACT

A mechanically flexible, transparent, rectifying and photosensitive organic-inorganic heterogeneous p-n junction is demonstrated on a plastic substrate. Hexagonally patterned n-type single-crystalline silicon nanomembrane (SiNM), created from silicon-on-insulator (SOI) wafer, was complementally combined with a p-type pentacene layer to form a heterogeneous p-n junction. Excellent rectifying characteristics were obtained from the heterogeneous p-n diode. The diode also exhibits high photosensitivity at visible wavelengths with a photo-to-dark current ratio exceeding four orders, a responsivity of 0.94 mA/W and an external quantum efficiency of 21.9% at 633 nm wavelength. Over 75% peak transmittance in the visible spectrum was measured from the heterogeneous multilayer junction on a thick plastic substrate. Excellent mechanical bending characteristics were observed with up to 1.08% of strain applied to the diode. These results suggest that organic-inorganic heterogeneous integration could be a viable strategy to overcome the intrinsic limits of each individual material and thus enable a number of novel multifunctional applications.

Keywords: organic-inorganic heterojunction, flexible photodetector, silicon nanomembrane, pentacene

INTRODUCTION

Heterogeneous integration of dissimilar materials has been pursued for several decades. The unique physical properties of heterojunctions have led to many advanced device structures and applications such as heterojunction/heterostructure transistors [1], lasers [2], and solar cells [3]–[6]. As of today, most heterojunctions were formed either solely with inorganic semiconductors or solely with the organic semiconductors. Organic-inorganic hybrid materials have been explored by uniquely combining and engineering them at the molecular level [7-8]. However, limited p-n heterojunctions were made between organic and inorganic semiconductor materials [9-10]. Organic materials possess the advantages of processing ease (e.g., low temperature and spin coating, etc.), low cost, superior mechanical bending/stretching capability and and large-area applicability, but with poor charge carrier properties. However, most organic semiconductors exhibit p-type, while the n-type is more challenging to synthesize and often not stable. Owing to this reason, organic p-n junction devices often degrade very fast [11-12] when they are exposed to unfavorable environments. Therefore, many organic semiconductor applications can only use the p-type materials.

On the other hand, inorganic semiconductors, particularly single crystalline materials, although are more expensive, more difficult to be applied to large area and have limited mechanical bendability, they have superior charge carrier properties and can be formed into either n-type or p-type, both of high quality. These wafer based high quality rigid semiconductors used to be inaccessible for flexible electronics applications. However, recent advances of releasable and transfer printable single crystalline semiconductor nanomembranes (NMs), still inheriting the single crystal quality, [13-14] have enabled the inorganic semiconductors to be also applicable to flexible substrates.

In this paper, we present an approach to forming high performance organic and inorganic heterogeneous p-n junctions, based on organic semiconductors and inorganic NM semiconductors. We implemented the heterogeneous p-n junction by combining transferrable n-type single crystal silicon nanomembranes (SiNM) and p-type pentacene on a plastic substrate using a simple fabrication process.

EXPERIMENT

Figure 1 schematically illustrates the representative processing steps for fabricating the single crystalline Si and pentacene heterojunction diodes. The fabrication began with a silicon-on-insulator (SOI) wafer (Soitec UnibondTM with a n-type 340 nm top Si layer with doping level of $1.0-4.0 \times 10^{15}/cm^3$) (Fig. 1(a)). Heavily doped regions were formed on the template layer for an ohmic contact via phosphorous diffusion. The drive-in diffusion process was carried out at 800℃ by rapid thermal annealing (Fig. 1(b)). After finishing photolithography and reactive ion etching

(RIE) steps for defining the hexagonal mesh on the top of Si template layer, the 2 µm buried oxide layer of the SOI was undercut with hydrofluoric acid. The released top Si layer forms SiNM and is ready to be transferred to a foreign substrate (Fig. 1(c)). By utilizing an elastomeric polydimethylsiloxane (PDMS) stamp, the released SiNM was picked up and transferred to a 250 µm thick polyethylene terephthalate (PET) substrate that was pre-coated with 1.5 µm SU-8 as an adhesives layer (Fig. 1(d)). On top of the transferred SiNM, 70 nm thick pentacene thin film was thermally evaporated at room temperature (Fig. 1(e)), followed by metal evaporation of Ti/Au of 5 nm/350 nm for electrodes (Fig. 1(f)).

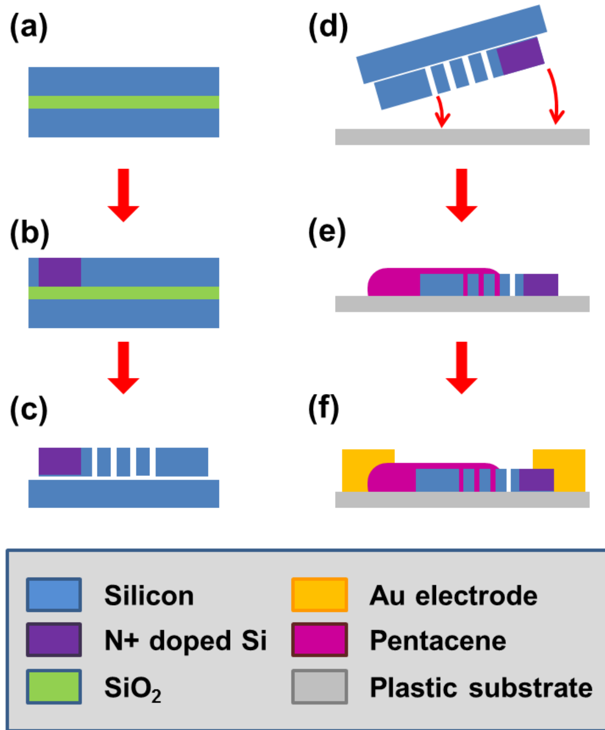

Figure. 1. Schematic illustration of the fabrication process flow of organic-inorganic heterogenous photodetector

RESULT AND DISCUSSION

The measured forward and reverse bias I-V characteristics of the Si-pentacene heterojunction diode are shown in Figure 2(a). The diode shows good rectifying behavior. To model the diode, we express the I-V using the non-ideal diode equation, which includes the associated series resistance, based on the thermionic emission theory,

$$I = A_{eff} \cdot A^{*} \cdot T^{2} \cdot \exp\left(\frac{-q\emptyset_B}{kT}\right) \cdot \exp\left(\frac{q(V-IR)}{nkT}\right) \qquad (1)$$

where V is the applied voltage, q is the electronic charge, n is the ideality factor, k is the Boltzmann constant, T is the temperature, R is the series resistance, A_{eff} is the active device area, A* is the effective Richardson constant (112 A/cm^2 K^2 for n-type silicon) and ϕB is the barrier height. At higher voltages, series resistance becomes dominant in the diode I-V characteristics. To analyze the series resistance effect, equation (1) can be rearranged in terms of current density as [15]

$$V = R \cdot A_{eff} \cdot J + n \cdot \emptyset_B + \left(\frac{n}{q/kT}\right) \cdot ln\left(\frac{J}{A^{**} \cdot T^{2}}\right) \qquad (2)$$

To calculate the series resistance and the ideality factor, equation (2) can be differentiated with respect to the current density (J). The barrier height of junction can be defined by an equation (3)

$$F(J) = R \cdot A_{eff} \cdot J + n \cdot \emptyset_B \qquad (3)$$

where is the barrier height. The calculated series resistance R is 98,720 ohm and the ideality factor is found to be 1.94. This number is close to the ideality factor (n = 1.89) directly extracted from the measured I-V curve (Figure 2(a), in dark). The barrier height of the diode was determined using the plot of F(J) versus J and found to be 1.03 eV under equilibrium. Since pentacene is relatively an inefficient hole injector, we observed low current density (1.4 mA/cm^2) and high series resistance. The higher value of ideality factor may be also partially explained by the presence of native oxide on Si and/or possible degradation of pentacene layer.

The photosensitivity results of the diode are also shown in Figure 2(a). The measured dark current is lower than 3×10^{-10} A up to -5V bias and is weakly dependent on the reverse-bias voltage. The photocurrent under the illumination of the three visible lasers (red: 633 and green: 532 nm) were also shown for comparison with the dark current. As a photodetector, the diode, biased at -5 V, exhibits a photocurrent of 4.7×10^{-6} A and 2.1×10^{-6} A under the illumination of the red and green lasers. For case of the 532 nm laser illumination, the ratio between the photo and the dark current is about 1.8×10^{4} and the calculated photo responsivity is 0.94 mA/W at -5 V.

Since the substrates and all the device materials are flexible, the bending effects on the characteristics of the diode were characterized. Figure 2(b) shows the I-V characteristics of the diode as a photodetector with 633 nm incident light under bending conditions as a function of the bending strain. The external quantum efficiency was 21.9 % and the photo responsivity was 0.94 mA/W at -5 V. Under bending with the application of 1.08 % strain, the photocurrent slightly increases from 4.7×10^{-6} A to 5.4×10^{-6} A . The corresponding external quantum efficiency and photo responsivity increase up to 25.1 % and 1.08 mA/W, respectively, at -5 V bias.

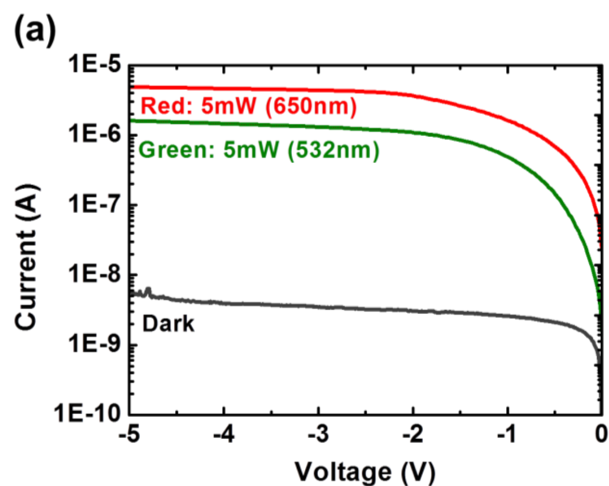

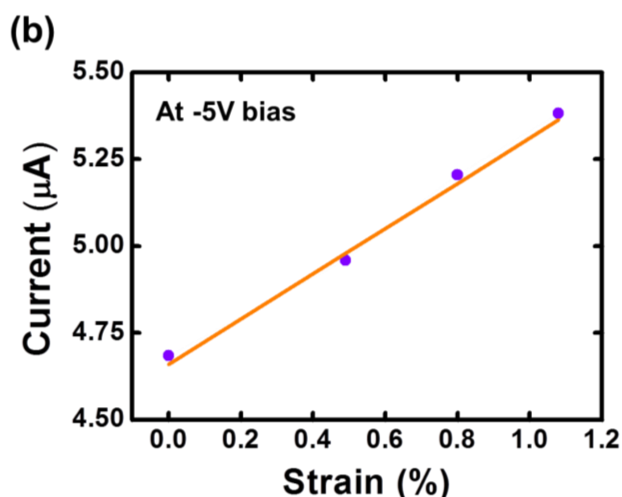

Figure. 2. (a) Current-voltage characteristics of the diode in dark and under illumination of lasers with wavelengths of 532 and 633 nm, respectively. The laser light intensity is 5 mW. (b) Measured photocurrent of the diode under different bending strain.

The transmittance spectrum of the diode sample including its 250 μm PET/SU-8 and Pentacene/SU-8/PET for comparison is shown in Figure 3. With such multiple layers that consists of a 250 μm thick PET, an average transmittance of 63% in the visible range (400-750 nm) was still measured. Using the same configuration, but without the SiNM layer, an average transmittance of 69 % in the visible range was observed. The small degradation of transmittance with the presence of the SiNM is ascribed to the patterned hollow hexagonal structure in the SiNM, besides its thinness. Evidently, the Si-pentacene heterostructure itself displays high transparency. An optical image of the diode sample is shown in inset of Figure 3.

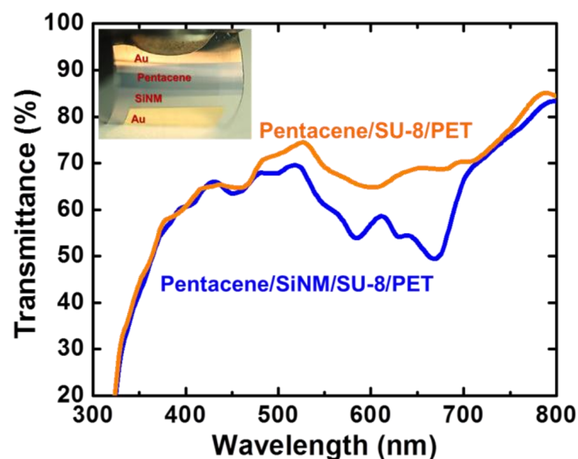

Figure. 3. (a) The transmittance spectra of a pentacene on SU-8 coated PET and the final device structure consisting of pentacene/SiNM/SU-8/PET. The inset is an optical image of the sample showing its transparency and bendability.

CONCLUSION

We demonstrated a flexible, transparent, rectifying and photosensitive organic-inorganic p-n heterojunction by complementally combining flexible single-crystal n-type silicon nanomembrane and p-type pentacene layer on a plastic substrate. The successful functional integration between organic and special form inorganic materials suggests that such heterogeneous integration approach could be a viable strategy to overcome the intrinsic limits of each individual material. A number of novel biomedical sensing and energy applications may be enabled in the future.

REFERENCES

[1] Ma Zhenqiang, S. Mohammadi, Lu Liang-Hung, P. Bhattacharya, L. P. B. Katehi, S. A. Alterovitz, and G. E. Ponchak, Microwave and Wireless Components Letters, IEEE 11 (7), 287 (2001).

[2] H. Morkoc and S. N. Mohammad, Science 267 (5194), 51 (1995).

[3] M. Estrada Y. Matsumoto , J. C. Nolasco in Photovoltaic Specialists Conference, 2008. PVSC '08. 33rd IEEE (San Diego, CA, USA, 2008).

[4] Sushobhan Avasthi, Stephanie Lee, Yueh-Lin Loo, and James C. Sturm, Advanced Materials 23 (48), 5762 (2011).

[5] Akira Tada, Yanfang Geng, Qingshuo Wei, Kazuhito Hashimoto, and Keisuke Tajima, Nat Mater 10 (6), 450 (2011).

[6] David M. Huang, Scott A. Mauger, Stephan Friedrich, Simon J. George, Daniela Dumitriu-

LaGrange, Sook Yoon, and Adam J. Moulé, Advanced Functional Materials 21 (9), 1657 (2011).
[7] D. B. Mitzi, K. Chondroudis, and C. R. Kagan, IBM Journal of Research and Development 45 (1), 29 (2001).
[8] C. R. Kagan, D. B. Mitzi, and C. D. Dimitrakopoulos, Science 286 (5441), 945 (1999).
[9] E. Katsia, N. Huby, G. Tallarida, B. Kutrzeba-Kotowska, M. Perego, S. Ferrari, F. C. Krebs, E. Guziewicz, M. Godlewski, V. Osinniy, and G. Luka, Applied Physics Letters 94 (14), 143501 (2009).
[10] B. N Pal, J. Sun, B. J Jung, E. Choi, A. G Andreou, and H. E Katz, Advanced Materials 20 (5), 1023 (2008).
[11] M. Rusu, J. Strotmann, M. Vogel, M. Ch Lux-Steiner, and K. Fostiropoulos, Applied Physics Letters 90 (15), 153511 (2007).
[12] Yanzhao Cheng, Guojia Fang, Chun Li, Longyan Yuan, Lei Ai, Bingruo Chen, Xingzhong Zhao, Zhiyuan Chen, Weibin Bai, and Caimao Zhan, Journal of Applied Physics 102 (8), 083516 (2007).
[13] Lei Sun, Guoxuan Qin, Jung-Hun Seo, George K. Celler, Weidong Zhou, and Zhenqiang Ma, Small 6 (22), 2473 (2010).
[14] Dae-Hyeong Kim, Nanshu Lu, Rui Ma, Yun-Soung Kim, Rak-Hwan Kim, Shuodao Wang, Jian Wu, Sang Min Won, Hu Tao, Ahmad Islam, Ki Jun Yu, Tae-il Kim, Raeed Chowdhury, Ming Ying, Lizhi Xu, Ming Li, Hyun-Joong Chung, Hohyun Keum, Martin McCormick, Ping Liu, Yong-Wei Zhang, Fiorenzo G. Omenetto, Yonggang Huang, Todd Coleman, and John A. Rogers, Science 333 (6044), 838 (2011).
[15] S. K. Cheung and N. W. Cheung, Applied Physics Letters 49 (2), 85 (1986).

---

a) †These authrs contributed equally to this work
b) Authors to whom correspondence should be addressed.
Electronic addresses: bkju@korea.ac.kr and mazq@engr.wisc.edu